Density functional investigation of intermolecular effects on ^{13}C NMR chemical-shielding tensors modeled with molecular clusters

Sean T. Holmes,[1] Robbie J. Iuliucci,[2] Karl T. Mueller,[3,4] and Cecil Dybowski[1]
[1]*Department of Chemistry and Biochemistry, University of Delaware, Newark, Delaware 19716, USA*
[2]*Department of Chemistry, Washington and Jefferson College, Washington, Pennsylvania 15301, USA*
[3]*Department of Chemistry, Pennsylvania State University, University Park, Pennsylvania 16802, USA*
[4]*Environmental Molecular Sciences Laboratory, Pacific Northwest National Laboratory, Richland, Washington 99352, USA*

(Received 15 August 2014; accepted 14 October 2014; published online 29 October 2014)

A quantum-chemical method for modeling solid-state nuclear magnetic resonance chemical-shift tensors by calculations on large symmetry-adapted clusters of molecules is demonstrated. Four hundred sixty five principal components of the ^{13}C chemical-shielding tensors of 24 organic materials are analyzed. The comparison of calculations on isolated molecules with molecules in clusters demonstrates that intermolecular effects can be successfully modeled using a cluster that represents a local portion of the lattice structure, without the need to use periodic-boundary conditions (PBCs). The accuracy of calculations which model the solid state using a cluster rivals the accuracy of calculations which model the solid state using PBCs, provided the cluster preserves the symmetry properties of the crystalline space group. The size and symmetry conditions that the model cluster must satisfy to obtain significant agreement with experimental chemical-shift values are discussed. The symmetry constraints described in the paper provide a systematic approach for incorporating intermolecular effects into chemical-shielding calculations performed at a level of theory that is more advanced than the generalized gradient approximation. Specifically, NMR parameters are calculated using the hybrid exchange-correlation functional B3PW91, which is not available in periodic codes. Calculations on structures of four molecules refined with density plane waves yield chemical-shielding values that are essentially in agreement with calculations on clusters where only the hydrogen sites are optimized and are used to provide insight into the inherent sensitivity of chemical shielding to lattice structure, including the role of rovibrational effects. © *2014 AIP Publishing LLC*.
[http://dx.doi.org/10.1063/1.4900158]

I. INTRODUCTION

Nuclear magnetic resonance (NMR) chemical-shift tensors are a powerful gauge of local electronic geometry.[1,2] A variety of one- and two-dimensional methods for obtaining ^{13}C chemical-shift tensors from the spectra of solids can be found in the literature. It has become routine to acquire these data with accuracies as high as ± 1 ppm.[3–6] The full chemical-shift tensor (including the orientation of its principal axes relative to crystal axes) may be obtained from experiments on a single-crystal sample. If external knowledge of symmetry requirements gives information on the orientation of the principal axes, it is sometimes possible to associate principal components obtained from analysis of a powder with particular crystal axes, but in general, the orientational information is not available from spectra of powders. The principal components of the chemical-shift tensor contain important information regarding the local structure of the molecule in which the nucleus resides, as well as information on extended spatial relationships between molecules in the solid state.[7] Despite this strong dependence on structure, it remains difficult to interpret data in terms of local structure without quantum chemical models.[8–10] Experimental chemical shifts are often correlated with calculated magnetic shieldings to gain a deeper insight into a material's local structure. The ever-increasing number of published solid-state ^{13}C chemical-shift measurements has been met with a corresponding demand for highly accurate computational models for calculating magnetic shielding in solids.[11]

Several effects are important when calculating NMR chemical shielding in a solid, which largely can be ignored in solution- or gas-phase systems.[12] Molecules maintain long-range spatial relationships with other molecules in the crystal lattice that are not averaged out by thermal motion. Individual molecules in a solid are often distorted from their idealized gas-phase structures by van der Waals' interactions, hydrogen bonding, and steric interactions with adjacent molecules. These effects may be observed as changes of bond lengths and angles, as bending in planar compounds, as fixing the orientation of a pendant group, or as any of a number of other differences from solution- and gas-phase structures. More than one unique molecule may be present in the asymmetric unit of a solid, giving rise to more nuclear sites than otherwise would be predicted on the basis of a unique molecule considered in isolation. Structural polymorphism may exist in which the material has multiple stable crystalline phases that depend on the history of the sample, each polymorph having a unique set of magnetic shieldings due to differences in the local structure.

For a molecular solid, the shielding experienced at a nuclear site may be assumed to be due to internal currents in the molecule or to the effects of currents external to the molecule. Historically, many studies have focused solely on internal currents due to the cost of modeling the lattice in shielding calculations. Studies examining intermolecular effects in heavy-nucleus-containing compounds, where the range of possible chemical shifts is much larger than that of carbon, illustrate how important intermolecular and lattice effects can be.[13] In cases where intermolecular effects are expected to be small, their contributions must still be considered to ensure that the model is an accurate representation of the material.

A common approach to calculation of magnetic shielding in a solid is to use periodic-boundary conditions (PBCs), such as that employed in the gauge-invariant-projector-augmented-wave (GIPAW) method. In this method, use of Bloch's theorem provides translational symmetry to the wave function.[14] The GIPAW method is demonstrably superior to isolated-molecule models for predicting ^{13}C NMR magnetic-shielding tensors, as has been shown in a variety of organic systems.[15] A review of applications of the GIPAW method has recently been presented.[16] The majority of calculations based on the GIPAW approach have been performed within the formalism of the generalized-gradient approximation (GGA). Modern hybrid functionals that incorporate a portion of Fock exchange are known to improve calculations of atomization and ionization energies.[17] Inclusion of this term also improves the quality of computed spectroscopic properties, including NMR parameters, due to the treatment of the band-gap problem.[18–20] However, Fock exchange is difficult to implement in plane-wave calculations due to the appearance of a singularity that slows convergence.[21]

The NMR chemical shift is largely a local phenomenon, and the use of periodic calculations comes with the tradeoff of a limited selection of model chemistries to describe these local effects, notably hybrid exchange-correlation functionals. Popular techniques such as nucleus-independent chemical shielding (NICS) cannot be performed in a periodic calculation, nor can spin-orbit terms be incorporated into the Hamiltonian as implemented by models such as the zero-order regular approximation (ZORA). Additionally, it is difficult to calculate the magnitude of intermolecular effects in plane-wave calculations because any comparison with an isolated molecule is tenuous, due to a lack of correspondence between basis sets in the two methodologies.

Cluster models emphasize the importance of local rotational symmetry by employing gauge-including atomic orbitals (GIAOs).[22–25] Magnetic-shielding components obtained from a cluster representing a portion of the solid state can be compared directly to an isolated molecule to assess the importance of intermolecular effects. Cluster calculations have the advantage that they are not limited to periodic systems and can be applied to amorphous solids, nanostructures, surfaces, biological systems, and gas-phase conglomerations of molecules.[26] All of these considerations make an exploration of the advantages and limitations of cluster methodologies of fundamental importance.

An early example of NMR parameters calculated using clusters is the prediction of ^{1}H shifts in $(H_2O)_{17}$ clusters.[27] Later analyses expanded cluster methodologies to solid materials. Another early study examined ^{23}Na isotropic shifts in several sodium oxides.[28] Tossell *et al.* have investigated lattice effects on ^{15}N and ^{23}Na in various materials including silicates and aluminosilicates.[29–31] ^{27}Al and ^{29}Si shieldings in zeolites have also been addressed in this manner.[32,33] Cluster methods were employed more recently in a study of ^{19}F magnetic shielding in inorganic fluorides.[34,35] Our laboratory has examined the use of clusters for calculating ^{199}Hg and ^{207}Pb shifts in a large variety of materials.[13,36,37] Orendt *et al.* have calculated ^{13}C chemical shielding for an acetate adduct of cadmium.[38] However, the study of structural effects on NMR parameters of organic solids has been confined largely to materials of biological importance. In a survey of crystalline amino acids, Zheng *et al.* calculated the effects of hydrogen bonding on chemical shielding.[39] In their study, the two nearest amino acids were replaced by NH_3 groups to reduce computational cost. The calculation of properties of small clusters, sometimes employing molecular fragments, has been applied to ^{15}N chemical shielding.[40–42] In general, the effects of nearest neighbors have been explored in cases where neighboring molecules are involved in hydrogen-bonding or π-stacking interactions. Chen and Zhan performed calculations which included between six and nine complete molecules to represent the local structure of a solid. With these models they were able to achieve better agreement with experiment than was possible with earlier small-cluster methods.[43]

Cluster models have associated problems, the most prominent among these being the extent and termination of the cluster.[44] Clusters must be designed to reflect the lattice structure around the NMR-active nucleus. This is often done by judiciously selecting several nearby molecules which are believed to influence the local electronic environment strongly. To reduce the computational cost, molecular fragments are sometimes used as a replacement for nearby molecules. This technique may introduce computational artifacts due to the inability to stabilize the charge on dangling bonds. Furthermore, including only a handful of the neighboring molecules or molecular fragments in the calculation can introduce symmetry constraints that are not present in the actual structure.

This study provides benchmark calculations of a wide variety of ^{13}C chemical-shielding tensors in organic solids, where the crystalline lattice is modeled with a molecular cluster. The results demonstrate the size and symmetry conditions that must be met for the cluster to predict the NMR properties of the solid state accurately. A systematic approach for incorporating intermolecular effects into chemical-shielding calculations performed at a level of theory more advanced than the generalized gradient approximation is presented.

II. THEORY AND COMPUTATIONAL DETAILS

A. Theory of magnetic shielding

Magnetic shielding (sometimes called chemical shielding to indicate its connection to the chemical shift) refers to the screening field experienced at a nuclear site due to interactions with induced electronic currents.[45,46] The magnitude of

this interaction is strongly dependent on the local electronic environment.[47] Chemical shielding is formally defined as a second-rank tensor of the form

$$\sigma_{ij} = \left.\frac{\partial^2 E}{\partial \boldsymbol{\mu}_i \partial \mathbf{B}_j^{\mathbf{ext}}}\right|_{\boldsymbol{\mu}=0,\, \mathbf{B}^{\mathbf{ext}}=0}. \quad (1)$$

In Eq. (1), $\boldsymbol{\mu}$ is the nuclear magnetic moment, $\mathbf{B}^{\mathbf{ext}}$ is the external field, E is the total energy of the system derived from the full Hamiltonian including electronic and nuclear terms, and the subscripts i and j denote axes which describe the orientation of the molecular structure in the magnetic field. The full tensor has nine unique elements; however, if the tensor is symmetric, or the antisymmetric components are negligibly small (as is often considered to be the case, but not guaranteed), the number of unique tensor elements is reduced to six. Referred to a set of coordinates called the principal-axis system, the chemical-shielding tensor is diagonal and is characterized by the three principal chemical-shielding components. The principal components are ranked using the frequency-ordered convention, such that $\sigma_{11} \leq \sigma_{22} \leq \sigma_{33}$. The isotropic shielding (σ_{iso}) is the average of the three principal components and contains only average structural information. Knowledge of the principal components provides additional information about the structure. Comparison of calculated and experimental chemical-shift principal values offers a more stringent test of the model than the isotropic shifts alone.

Chemical shielding is evaluated as a three-center integral of the general form

$$\langle \phi_a | \hat{L}_k | \phi_b \rangle \neq 0, \quad (2)$$

where ϕ_a and ϕ_b are one-electron orbitals and $\hat{L}_k$ is an angular-momentum operator with respect to either the magnetic field or the nuclear origin.[48,49] The angular momentum operators belong to the same irreducible representations as the rotational operators of group theory ($\hat{R}_k$):[50]

$$\Gamma(\hat{L}_k) = \Gamma(\hat{R}_k). \quad (3)$$

The effect of $\hat{L}_k$ operating on an orbital can be visualized as the rotation of the orbital around a particular axis. Qualitatively, the point group of a molecule or the space group of a solid can be used to predict the symmetry-allowed mixing of orbitals that contribute to the calculated shielding. This fact suggests a strong dependence on both localized and extended symmetry operations, which must be considered when designing a cluster to represent the solid state. In a crystalline solid, the simplest repeating unit is given by the space group. For a cluster to represent the solid state sufficiently well, all symmetry elements of the space group must be present in the cluster.

The simplest method to take into account space-group symmetry in a cluster model is to preserve all symmetry requirements from the perspective of a single molecule located at the center of the cluster. Thus, a material belonging to a spherical space group would be represented by a cluster where the central molecule is surrounded by a spherical shell of peripheral molecules.

B. Materials

In this study, we selected 24 organic materials that have both accepted single-crystal neutron diffraction structures and measurements of the principal components of the ^{13}C chemical-shift tensors with small associated uncertainties. The majority of chemical-shift principal components in this study have been measured to within ±1.0 ppm and the maximum uncertainty of any single value is ±4.1 ppm. The specific materials investigated in this study are methyl α-D-glucopyranoside,[51,52] methyl α-D-mannopyranoside,[51,52] methyl α-D-galactopyranoside monohydrate,[51,53] methyl β-D-galactopyranoside,[51,54] methyl β-D-xylopyranoside,[51,55] sucrose,[56,57] α-L-rhamnose monohydrate,[58,59] β-D-fructopyranose,[60,61] α-glycine,[62,63] γ-glycine,[64,65] L-alanine,[66,67] L-serine monohydrate,[68,69] L-asparagine monohydrate,[70,71] L-threonine,[72,73] oxalic acid dihydrate,[74,75] squaric acid,[76,77] naphthalene,[78,79] durene,[80,81] triphenylene,[82,83] acenaphthene,[84,85] pentaerythritol,[86,87] adenosine,[88,89] acetaminophen (form I),[90,91] and ibuprofen (form I).[92,93] These materials, which include saccharides, aromatic rings, amino acids, nucleosides, active pharmaceutical ingredients, etc., were chosen to represent a wide variety of local electronic environments. Altogether, 465 chemical-shift principal components have been considered. Of these, 258 are for nuclei in aliphatic environments, 165 are for nuclei in aromatic environments, and 42 are for nuclei in carboxylic environments. Several of these materials have been used as model compounds in previous work examining the efficacy of various exchange-correlation functionals and *ab initio* methods[94] or basis sets[95] to model the chemical shift, or as case studies illustrating the importance of lattice effects on the chemical shift in periodic plane-wave calculations.[15,96]

C. Computational details

Beginning with neutron structures, proton positions were optimized on an isolated molecule at the B3LYP level of theory using the 6-31G(d) basis set.[97–99] In the partial geometry optimizations, all heavy atoms remained frozen in their experimental positions, as did all hydrogen atoms participating in intermolecular hydrogen bonding. This feature of the optimization was especially important for saccharides, which are distorted from the ideal staggered conformation. Optimizing these sites would have eliminated this important structural feature. The refined coordinates were used to build large clusters of molecules to represent the local solid-state environment around a single molecule. Table I contains a summary of all materials investigated, their space groups, and the compositions of the model clusters.

For reasons discussed below, periodic plane-wave geometry optimizations were performed on adenosine, acetaminophen, ibuprofen, and α-glycine using the energy-minimization method of Broyden, Fletcher, Goldfarb, and Shanno, as implemented in the CASTEP module of MATERIALS STUDIO 6.1 by Accelrys Software, Inc.[100] Optimizations were performed at the PBE/ultra-fine level of theory with a plane-wave cutoff energy of 610 eV and a k-point spacing of

TABLE I. Crystal structures and cluster compositions for materials examined in this study.

Compound	Space group	Cluster composition
L-alanine	$P2_12_12_1$	$13C_3H_7NO_2$
L-asparagine monohydrate	$P2_12_12_1$	$15C_4H_8N_2O_3 \cdot 6H_2O$
L-serine monohydrate	$P2_12_12_1$	$11C_3H_7NO_3 \cdot 8H_2O$
L-threonine	$P2_12_12_1$	$15C_4H_9NO_3$
Methyl α-D-galactopyranoside monohydrate	$P2_12_12_1$	$15C_7H_{14}O_6 \cdot 6H_2O$
Methyl α-D-glucopyranoside	$P2_12_12_1$	$15C_7H_{14}O_6$
Methyl α-D-mannopyranoside	$P2_12_12_1$	$13C_7H_{14}O_6$
Methyl β-D-galactopyranoside	$P2_12_12_1$	$15C_7H_{14}O_6$
Triphenylene	$P2_12_12_1$	$15C_{18}H_{12}$
β-D-fructopyranose	$P2_12_12_1$	$15C_6H_{12}O_6$
Acenaphthene	$Pcm2_1$	$15C_{12}H_{10}$
Adenosine	$P2_1$	$15C_{10}H_{13}N_5O_4$
Methyl β-D-xylopyranoside	$P2_1$	$13C_6H_{11}O_5$
Sucrose	$P2_1$	$13C_{12}H_{22}O_{11}$
α-L-rhamnose monohydrate	$P2_1$	$15C_6H_{12}O_5 \cdot 6H_2O$
Acetaminophen	$P2_1/a$	$15C_8H_9NO_2$
Durene	$P2_1/a$	$15C_{10}H_{14}$
Naphthalene	$P2_1/a$	$13C_{10}H_8$
Ibuprofen	$P2_1/c$	$15C_{13}H_{18}O_2$
Squaric acid	$P2_1/c$	$17C_4H_2O_4$
Oxalic acid dihydrate	$P2_1/n$	$15C_2O_4H_2 \cdot 20H_2O$
α-glycine	$P2_1/n$	$15C_2H_5NO_2$
γ-glycine	$P3_2$	$15C_2H_5NO_2$
Pentaerythritol	$I\bar{4}$	$13C_5H_{12}O_4$

0.07 Å^{-1}.[101] The unit cell dimensions remained fixed during the structural refinements because these parameters are well-known from experiment.

Chemical-shielding tensors were computed using the GIAO method with the B3PW91 functional, Becke's three-parameter hybrid functional where the non-local correlation is provided by the Perdew-Wang-91 gradient-corrected functional.[102] Calculations were performed using a two-layer approach, in which a more flexible basis set was given to the molecule of interest (the central molecule of the cluster) than was given to the neighboring molecules in the cluster. This approach is justified by the relative importance of intra- and intermolecular effects on ^{13}C chemical shielding. Dunning's correlation-consistent basis set cc-pVTZ was used for the central molecule and cc-pVDZ was used for peripheral molecules.[103] Shielding calculations and non-periodic geometry optimizations were performed using the GAUSSIAN 09 software package.[104]

III. DISCUSSION OF RESULTS

A. Partial optimizations of hydrogen positions

Careful attention must be paid to experimental conditions under which crystal structures and NMR chemical shifts are obtained. Computational refinements of crystal structures are often necessary to ensure that meaningful NMR parameters can be extracted. The method by which the structure was determined should dictate the method used to refine the experimental structure. It has been observed that X-ray diffraction cannot resolve the positions of hydrogen atoms with a level of accuracy that allows chemical shieldings to be computed reliably, although partial optimizations involving only proton positions, or full optimizations involving all atoms, can overcome experimental uncertainty to some extent.[51,86] Structures obtained from neutron diffraction generally locate the positions of hydrogens more accurately than those obtained from X-ray diffraction.

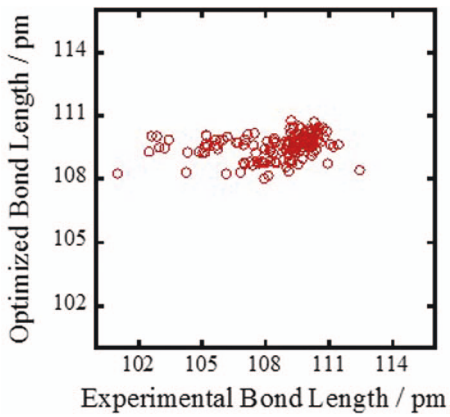

FIG. 1. Experimental neutron diffraction C–H bond lengths versus B3LYP/6-31G(*d*) optimized bond lengths.

We have addressed the positioning of hydrogen atoms by using neutron diffraction structures as a starting point. To minimize differences between the experimental methodologies, the positions of hydrogen centers that do not participate in hydrogen bonding were optimized. As expected, the geometry optimizations mostly resulted in small repositionings of hydrogens, with the largest deviations being for mobile methyl groups, which are usually rotated by several degrees and significantly lengthened. Fig. 1 shows the correlation between the experimental and B3LYP/6-31G(*d*) optimized C-H bond lengths. A significant amount of variation is present in the neutron data (1.01–1.13 Å) whereas the optimized structures consistently yield values between 1.08 Å and 1.11 Å. Optimizing these positions appears to be a crucial step in removing experimental variability in the placement of hydrogens. From these results, it appears that dynamic effects involving the rotation of methyl groups lead to unreasonably short bond lengths for these functional groups.

B. Design of clusters

There are several important issues associated with solid-state NMR chemical-shielding calculations using clusters. The first issue concerns proper termination of the cluster. For a molecular solid, a cluster can be defined by a shell of adjacent molecules around one central molecule. Truncating the adjacent molecules to form molecular fragments may increase computational efficiency with little effect on the overall accuracy of the computed shielding, but it frequently introduces problems in self-consistent-field (SCF) convergence due to excess charge on dangling bonds. This procedure introduces artifacts into the calculation by creating unphysical changes to the local site symmetry around the nucleus. All calculations in

TABLE II. ^{13}C Principal chemical-shielding values for oxalic acid dihydrate as a function of cluster size.

Cluster composition	σ_{11} (ppm)	σ_{22} (ppm)	σ_{33} (ppm)	σ_{iso} (ppm)
$C_2O_4H_2$	−80.3	75.9	84.7	26.8
$3C_2O_4H_2 \cdot 6H_2O$	−72.8	56.8	78.4	20.8
$11C_2O_4H_2 \cdot 12H_2O$	−70.9	54.7	77.6	20.4
$15C_2O_4H_2 \cdot 20H_2O$	−69.4	51.9	77.0	19.8

this investigation were performed on clusters containing only complete molecules.

Another issue is convergence of chemical shielding with increasing cluster size. To assess this effect, we calculated the shielding of an isolated molecule and that of a molecule in a cluster as a function of cluster size to demonstrate that the calculated shieldings tend to converge to a constant set of values that are independent of the size of the cluster. At this limit, the cluster model can be said to represent the lattice structure sufficiently. Table II shows the effect of cluster size on the chemical-shielding principal components of oxalic acid dihydrate. Shielding tends to converge smoothly. In this example, much of the difference relative to the isolated molecule is retrieved in calculations on a cluster containing only three oxalic acid molecules and six water molecules. Convergence only appears to be achieved with the largest cluster (containing fifteen oxalic acid molecules and twenty water molecules). Clusters of intermediate sizes yield shieldings that lay between the two extremes. From this observation, it is clear that clusters must be large to account for intermolecular effects properly, as illustrated in Tables I and II.

A third aspect of solid-state shielding calculations is the difficulty of ensuring that the cluster reflects all symmetry elements associated with the space group of the material. Neglecting any symmetry element in forming the cluster causes the wave function to be constrained to a particular subgroup of the correct space group. The simplest cluster that can sufficiently account for all lattice effects must have a unique constitution that depends on the space group of the material. For example, the $P2_12_12_1$ space group maintains spherical symmetry around the central molecule. The elimination of any of the three C_2 rotational axes in the cluster reduces the symmetry to a subgroup with either oblate or prolate spheroidal symmetry. All example clusters from the $P2_12_12_1$ space group in this study contain between thirteen and fifteen complete molecules that maintain the symmetry. A cluster of β-D-fructopyranose molecules is shown in Fig. 2 as a representation of this space group.

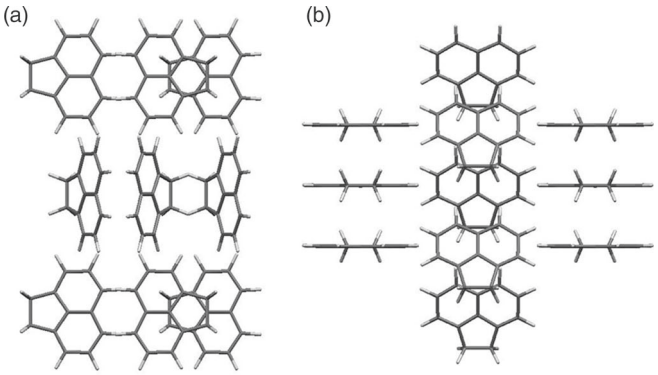

FIG. 3. Two orientations of a cluster of acenaphthene in the space group $Pmc2_1$ containing 15 molecules.

As a second example, acenaphthene belongs to the space group $Pmc2_1$, which has a single C_2 rotational axis and two mirror planes. Fig. 3 shows two orientations of a model cluster that contains 15 complete acenaphthene molecules and maintains the symmetry. A different σ_v plane is apparent in each panel and the C_2 axis can be seen in both.

The $P2_1$ space group is a subgroup of $P2_12_12_1$ and $Pcm2_1$, which has only one C_2 axis and no other rotational symmetry elements. Shown in Fig. 4 is a cluster built from 13 molecules of methyl β-D-xylopyranoside that maintains the symmetry.

As a final example, the $P3_2$ space group contains C_3 and C_3^2 elements as shown in Fig. 5 for α-glycine. The cluster is built from 15 complete molecules and maintains the proper symmetry. C_3 rotational axes lie between the molecules.

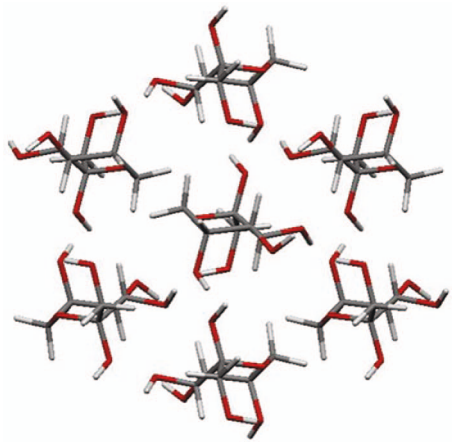

FIG. 2. Cluster of β-D-fructopyranose in the space group $P2_12_12_1$ containing 15 molecules.

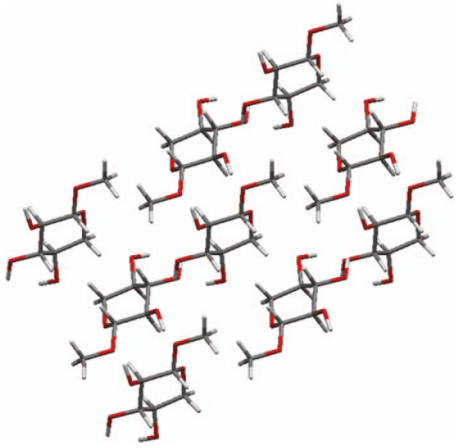

FIG. 4. Cluster of methyl β-D-xylopyranoside in the space group $P2_1$ containing 13 molecules.

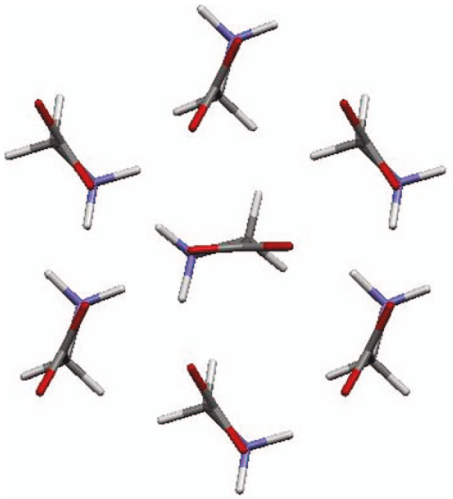

FIG. 5. Cluster of γ-glycine in the space group $P3_2$ containing 15 molecules.

C. Chemical shielding artifacts from cluster design

Artifacts may be introduced into a computational result by designing a cluster that does not maintain the symmetry elements of the crystalline space group. To illustrate this point, we present calculated chemical-shielding principal components for both carbon sites of pentaerythritol. Pentaerythritol belongs to the $I\bar{4}$ space group, which contains C_2, S_4, and $S_4{}^3$ symmetry elements. The chemical shielding from a model having the appropriate symmetry contains a twofold degeneracy of the principal values for the quaternary carbon site. When the symmetry is not fully realized, the principal values differ by a sizable amount, as seen in Table III.

The two clusters for which the data in Table III were calculated were designed from the diffraction structure (Fig. 6). The first cluster contained 13 molecules in a manner that preserved all symmetry elements of the crystalline space group. The second cluster was designed from only nine molecules, with the effect of removing the inversion center inherent in the crystalline space group. This smaller cluster is a quasi $-$ $I\bar{4}$ cluster, reflecting the difference from the actual crystalline symmetry. As is clearly evident in Table III, calculations on the first ($I\bar{4}$) cluster predict the degeneracy of the quaternary carbon, whereas calculations on the second cluster do not.

TABLE III. Calculated chemical-shift tensors for pentaerythritol using clusters with the experimental crystalline space group ($I\bar{4}$) and a space group of reduced symmetry (quasi $-$ $I\bar{4}$).

	Model	$\delta_{11} - \delta_{iso}$[a] (ppm)	$\delta_{22} - \delta_{iso}$[a] (ppm)	$\delta_{33} - \delta_{iso}$[a] (ppm)
Site A	Expt.	9.8	-4.9	-4.9
	Quasi $-$ $I\bar{4}$	12.5	-4.8	-7.7
	$I\bar{4}$	9.6	-4.8	-4.8
Site B	Expt.	33.8	9.4	-43.2
	Quasi $-$ $I\bar{4}$	34.1	12.0	-46.1
	$I\bar{4}$	36.0	8.7	-44.7

[a]Differences between calculated chemical shifts are reported as differences in calculated chemical shieldings, with opposite sign.

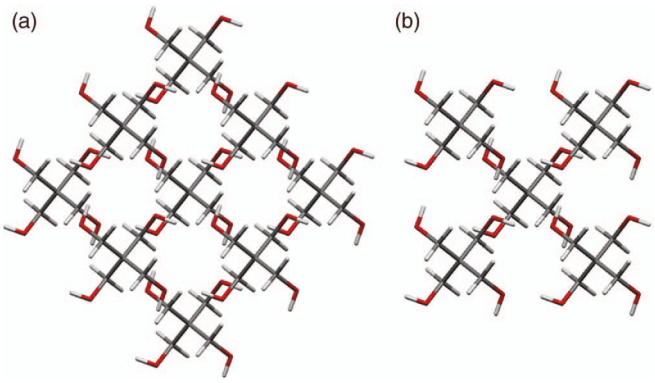

FIG. 6. Two example clusters of pentaerythritol. Cluster A is built from 13 complete molecules and maintains all of the symmetry elements of the $I\bar{4}$ space group. Cluster B is built from nine molecules and lacks several symmetry elements of the space group.

D. Locally dense basis sets

The use of locally dense, rather than balanced, basis functions allows calculations to be performed on large clusters, which otherwise would be prohibitively expensive. The use of locally dense basis functions in chemical-shielding calculations has been surveyed by Chesnut and co-workers.[105,106] They demonstrate that only small discrepancies appear between locally dense and balanced basis sets for ^{13}C, provided a sufficiently large basis set is employed in the dense region.

Some of the largest clusters in this study contain up to seven thousand Cartesian basis functions, although they use a smaller basis set for peripheral molecules. The ^{13}C chemical shielding of oxalic acid dihydrate, the smallest molecule in this study, serves as a basis for comparison because the chemical shielding of the carbon site can be calculated using the large basis set for all atoms. Differences in chemical-shielding principal components between balanced and locally dense basis functions are given in Table IV. The differences are under 1.5 ppm, indicating that the increase in computational efficiency outweighs the loss of accuracy associated with the smaller basis set. Oxalic acid dihydrate is expected to be an extreme case because the single unique carbon site is involved in a complicated network of intermolecular hydrogen bonds.

E. Linear regression to define reference chemical shielding

NMR experiments yield a shift in the frequency of the resonance of a particular chemical species relative to an arbitrary reference material, rather than the absolute shielding

TABLE IV. Comparison of locally dense and balanced basis sets for calculating the ^{13}C chemical shielding of oxalic acid dihydrate using the cluster $15C_2O_4H_2 \cdot 20H_2O$.

Method	σ_{11} (ppm)	σ_{22} (ppm)	σ_{33} (ppm)	σ_{iso} (ppm)
Locally dense	-69.4	51.9	77.0	19.8
Balanced	-67.9	50.9	77.8	20.3
Difference[a]	-1.5	1.0	-0.7	-0.5

[a]Locally dense shielding minus balanced shielding.

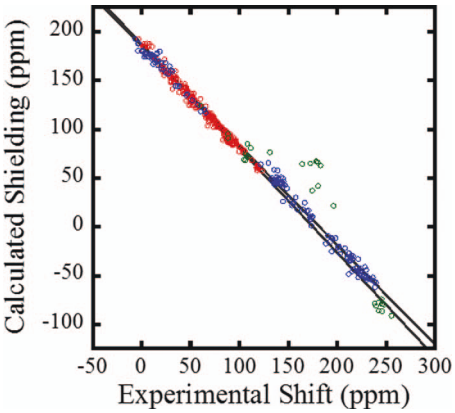

FIG. 7. Correlation plot for calculated principal chemical-shielding components versus experimental principal chemical-shift components for isolated-molecule models. Aliphatic carbons principal components are in red, aromatic principal components in blue, and carboxylic principal components are in green. Best-fit trend lines are indicated for the aliphatic and aromatic carbons.

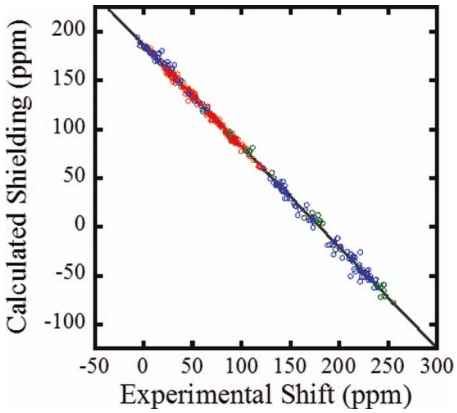

FIG. 8. Correlation plot for calculated principal chemical-shielding components versus experimental principal chemical-shift components for cluster models. Aliphatic carbons principal components are in red, aromatic principal components are in blue, and carboxylic principal components are in green. A unique best-fit correlation line considering all data is shown in black.

relative to the bare nucleus. For ^{13}C, chemical shifts are typically referenced to the resonance position of tetramethylsilane (TMS), whose principal components are all the same in solution because of the effective spherical symmetry caused by rapid motional averaging. The correlation between experimental chemical shifts ($\delta_{ii}^{exp.}$) and calculated chemical shieldings (σ_{ii}) is linear with a proportionality constant m, and an intercept that is the absolute chemical shielding of TMS,

$$\sigma_{ii} = m\delta_{ii}^{exp.} + \sigma_{\mathrm{TMS}}. \tag{4}$$

We use as a reference in our calculations the intercept derived from the linear regression of a correlation plot. Ideally, m should be -1, with deviations reflecting systematic flaws in the method of calculating the shielding tensor.[9] With knowledge of the reference shielding and slope, all chemical-shielding components can be expressed as their equivalents on the chemical-shift scale ($\delta_{ii}^{calc.}$), for comparison to experiment,

$$\delta_{ii}^{calc.} = \frac{\sigma_{ii} - \sigma_{TMS}}{m}. \tag{5}$$

In addition, to quantify the data scatter of the set of calculations, we use the root-mean-square deviation (RMSD) of the set,

$$RMSD = \sqrt{\frac{1}{N-2}\sum_{n=1}^{N}\left(\delta_{ii}^{calc.} - \delta_{ii}^{exp.}\right)^2}, \tag{6}$$

where N is the total number of chemical-shielding-tensor components.

Figs. 7 and 8 show correlation plots for the calculated chemical-shielding principal components versus experimental chemical-shift principal components. In Fig. 7, the results for the isolated-molecule models are displayed; in Fig. 8, the results of the cluster models are displayed. Table V gives the best-fit parameters for Eq. (4) for several different cases.

TABLE V. Linear-regression parameters for ^{13}C principal chemical-shielding values versus principal chemical-shift values for isolated molecules, clusters, and plane-wave optimized clusters.

Model	N-2[a]	Slope	σ_{TMS} (ppm)	RMSD (ppm)	Largest residual (ppm)
All					
Isolated		-1.010 ± 0.006	184.5 ± 0.8	9.5	62.6
Cluster	463	-1.035 ± 0.002	186.1 ± 0.3	3.4	17.2
Cluster, Opt.		-1.039 ± 0.002	186.4 ± 0.3	3.5	18.1
Aliphatic					
Isolated		-1.069 ± 0.007	187.2 ± 0.5	3.2	11.2
Cluster	256	-1.040 ± 0.005	186.0 ± 0.3	2.2	9.3
Cluster, Opt.		-1.052 ± 0.005	186.9 ± 0.4	2.3	9.0
Aromatic					
Isolated		-1.020 ± 0.005	185.3 ± 0.7	5.1	17.5
Cluster	163	-1.042 ± 0.004	187.3 ± 0.6	4.3	17.0
Cluster, Opt.		-1.043 ± 0.007	187.3 ± 0.7	4.6	18.3
Carboxylic					
Isolated		-1.06 ± 0.07	202 ± 13	25.9	52.0
Cluster	40	-1.03 ± 0.01	187 ± 2	4.5	9.2
Cluster, Opt.		-1.03 ± 0.01	186 ± 2	4.3	9.4

[a]Degrees of freedom.

In the isolated-molecule model, the correlation line for all results, regardless of carbon species, is

$$\sigma^{isolated} = 184.5 - 1.010\delta^{exp.} \quad (\text{RMSD} = 9.5\,\text{ppm}). \quad (7)$$

A similar correlation for the results of the cluster model gives

$$\sigma^{cluster} = 186.1 - 1.035\delta^{exp.} \quad (\text{RMSD} = 3.4\,\text{ppm}). \quad (8)$$

The RMSDs for these two models of 9.5 ppm (isolated-molecule model) and 3.4 ppm (cluster model) indicate that the cluster model is superior to the isolated-molecule model. The deviation from the ideal slope may reflect the choice of exchange-correlation functional and basis set employed in the calculation. The RMSD of the cluster model (3.4 ppm) represents approximately 1% of the possible ^{13}C chemical-shift dispersion, indicating that this method is a powerful, quantitative predictor of chemical-shift values. Every calculated value obtained by the cluster methodology agrees with experiment to within 5% of the possible chemical-shift range.

It is often assumed that one should correlate various species of carbons separately.[15] The set in this study consists of aliphatic, aromatic and carboxylic carbon species. In particular, it is assumed that different kinds of intermolecular interactions affect the chemical shielding at these sites differently. The data give the following results for aliphatic species:

$$\sigma^{isolated}_{aliphatic} = 187.2 - 1.069\delta^{exp.} \quad (\text{RMSD} = 3.2\,\text{ppm}), \quad (9)$$

$$\sigma^{cluster}_{aliphatic} = 186.0 - 1.040\delta^{exp.} \quad (\text{RMSD} = 2.2\,\text{ppm}). \quad (10)$$

Again, from comparison of the RMSDs of the two models, the cluster model appears to be better when considering the aliphatic chemical shifts. This change of 1.0 ppm is more impressive when one considers that it represents an average change of the calculated values in the correct direction for 258 principal components. The single largest deviation between the cluster models and isolated-molecule models for an aliphatic principal component is 13.6 ppm.

A similar analysis of the aromatic-carbon correlations gives

$$\sigma^{isolated}_{aromatic} = 185.3 - 1.020\delta^{exp.} \quad (\text{RMSD} = 5.1\,\text{ppm}), \quad (11)$$

$$\sigma^{cluster}_{aromatic} = 187.3 - 1.042\delta^{exp.} \quad (\text{RMSD} = 4.3\,\text{ppm}). \quad (12)$$

As with the aliphatic carbons, the comparison of the RMSDs shows that a cluster model is slightly better than the isolated-molecule model. As in the previous case, the decrease in the RMSD of 0.8 ppm reflects an average change over 165 principal components. Many individual values are relatively unchanged by the inclusion of intermolecular effects, whereas others, such as a σ_{22} value in the heterocyclic ring of adenosine, are changed up to 18.5 ppm.

The results for carboxylic carbons again demonstrate that the cluster model improves the predictive capability over the isolated-molecule model by these results:

$$\sigma^{isolated}_{carboxylic} = 202 - 1.07\delta^{exp.} \quad (\text{RMSD} = 25.8\,\text{ppm}), \quad (13)$$

$$\sigma^{cluster}_{carboxylic} = 187 - 1.03\delta^{exp.} \quad (\text{RMSD} = 4.5\,\text{ppm}). \quad (14)$$

The correlation for carboxylic sites has significant scatter about the correlation line for the case of an isolated-molecule model. The isolated-molecule model's RMSD of 25.8 ppm is substantially larger than the RMSD of 4.5 ppm for the cluster model. Additionally, the projected reference shift of 202 ppm is substantially different from the 187 ppm of the cluster model. This latter value is more in line with reference shieldings derived from other models.

The correlations for aliphatic, aromatic, and carboxylic carbons in the cluster model are sufficiently close that one may consider, within uncertainty, that they all follow a single correlation (Eq. (7)), with a low RMSD of 3.4 ppm. Perhaps this is the strongest indicator of the importance of incorporating the extended local structure into any calculations of the chemical-shielding tensor of a carbon site in the solid state.

It has been noted in GIPAW calculations that distinct types of carbon species have statistically different sets of linear-regression parameters.[15] This trend is notably absent in the results presented here, suggesting that symmetry-adapted cluster models using hybrid functionals provide an alternative to periodic models for calculation of solid-state NMR parameters.

F. Analysis of principal chemical-shielding components

Table VI summarizes the linear-regression parameters for each principal component of the aliphatic, aromatic, and carboxylic carbon species. In every case, the RMSDs of each principal component of each type of carbon demonstrate that the cluster model is closer to the experimental value than the corresponding component calculated with the isolated-molecule model, except for the σ_{11} values of the aromatic sites. For aliphatic species, deviations fall between 2.0 ppm (σ_{22}) and 2.3 ppm (σ_{11} and σ_{33}) for cluster models. However,

TABLE VI. Root-mean-square deviation between calculated and experimental chemical shifts modeled using isolated molecules, clusters, and plane-wave optimized clusters.

Model	All (ppm)	σ_{11} (ppm)	σ_{22} (ppm)	σ_{33} (ppm)	σ_{iso} (ppm)
All					
Isolated	9.5	7.0	14.2	4.6	3.6
Cluster	3.4	4.0	3.1	3.1	1.6
Cluster, Opt.	3.5	3.9	3.2	3.4	1.7
Aliphatic					
Isolated	3.2	3.4	2.9	3.3	3.2
Cluster	2.2	2.3	2.0	2.3	1.4
Cluster, Opt.	2.3	2.3	2.0	2.3	1.6
Aromatic					
Isolated	5.1	5.3	5.6	4.5	1.4
Cluster	4.3	5.6	3.6	3.8	1.5
Cluster, Opt.	4.6	5.4	3.8	4.5	1.6
Carboxylic					
Isolated	25.9	22.4	38.9	14.9	4.3
Cluster	4.6	4.6	5.4	4.2	3.0
Cluster, Opt.	4.5	4.2	5.5	4.2	3.0

TABLE VII. Mean-absolute-deviation between calculated chemical shielding of cluster models and isolated-molecule models.

	All (ppm)	σ_{11} (ppm)	σ_{22} (ppm)	σ_{33} (ppm)	σ_{iso} (ppm)
All	4.2	3.1	6.7	2.9	2.2
Aliphatic	2.3	2.0	1.9	2.8	1.7
Aromatic	3.3	2.0	5.0	2.8	1.4
Carboxylic	20.3	13.3	42.6	4.4	9.6

the RMSDs vary for the principal components of the aromatic and carboxylic sites. For aromatic carbons, the principal components are generally aligned such that σ_{11} is along the C–H bonding axis, σ_{22} is perpendicular to the bonding axis and in the plane of the ring, and σ_{33} is perpendicular to the plane of the ring. Of these values, σ_{22} seems to be most strongly influenced by intermolecular effects. For each carboxylic principal component the disagreement between experiment and calculation is greatly reduced by the inclusion of intermolecular effects, with RMSDs ranging between 4.2 ppm (σ_{33}) and 5.4 ppm (σ_{22}). The principal axes at carboxylic sites generally do not align with the bonding axes, leading to large changes for each principal component when intermolecular effects are incorporated. The most shielded element is generally aligned approximately perpendicular to the bonding axis, resulting in substantial differences for σ_{11} and σ_{22} and relatively small changes for σ_{33}.

The most significant discrepancies between isolated-molecule and cluster models are seen for σ_{22} values of carboxylic carbons. For example, σ_{22} of L-alanine differs from experiment by 62.6 ppm in the isolated-molecule model, but only by 6.7 ppm in the cluster model. σ_{11} and σ_{33} also differ from experiment for L-alanine by 17.0 ppm and 7.1 ppm in the isolated-molecule model, respectively, whereas in the cluster model there are deviations of only 3.5 ppm and 1.0 ppm, respectively. This fact further indicates that the isolated-molecule model does not give even a rough approximation of chemical shielding caused by the local structure of a carboxyl group in the solid state. For all cases where intermolecular hydrogen bonding is present, we find the same effects as are observed for L-alanine. Calculations on the amino acids employing isolated molecules predict that the ^{13}C chemical-shielding tensor for the carboxylic sites have nearly axial symmetry, whereas in cluster models, the carboxylic sites have nearly radial symmetry. The observed experimental results suggest that the radial symmetry is more appropriate.

The mean absolute deviations (MADs) between computed chemical-shielding values for isolated-molecule models and cluster models are given in Table VII. Deviations are given for each principal component of the chemical-shielding tensor. For aliphatic species, the three principal components deviate between 1.9 ppm and 2.3 ppm, indicating that no single direction is more highly influence by neighboring molecules than the others, on average. All calculated principal components agree equally well with experimental values. For the aromatic species, both σ_{11} and σ_{33} deviate by approximately the same amount (2.0 ppm to 2.8 ppm). However, σ_{22} deviates by 5.0 ppm, demonstrating that intermolecular effects tend to affect this particular principal component more than the others. For carboxylic carbons, the deviations are much larger, with the largest differences associated with σ_{22}. For this principal component, the principal axis for which lies near the intermolecular hydrogen-bonding axis, the MAD is 42.6 ppm. A much smaller MAD is seen for σ_{33} (4.4 ppm), the principal axis for which lies perpendicular to the bonding plane.

G. Effects of plane-wave structural refinement on shielding

The basis sets employed in this study are sufficiently large that substantial deviations from experimental values probably represent defects in the model used to compute chemical shieldings. The largest residuals calculated in this study are observed for acetaminophen, adenosine, ibuprofen, and α-glycine. Most anomalous results arise for the principal components in the plane of aromatic rings (when present in the structure). Several residuals are greater than 10 ppm. Because these residuals are much larger than those for other materials examined, we hypothesize that they may have arisen from rovibrational effects in the neutron diffraction structures.

Crystal-structure refinements have been monitored through agreement between calculated and experimental chemical-shift tensors.[90] Studies have shown that periodic density plane-wave optimizations produce modest improvements in predicted chemical shieldings over results obtained from unrefined coordinates determined by neutron diffraction in some cases. To examine if these effects are significant, we determined the effects of plane-wave optimizations on computed ^{13}C chemical-shielding principal components of acetaminophen, adenosine, ibuprofen, and α-glycine. The linear-regression results incorporating the optimized structures are included in Tables V and VI.

As before, linear-regression parameters are used to assess the fit of the distinct carbon species. The linear-regression parameters, for the data set comprising all principal components, are

$$\sigma^{cluster,opt.} = 186.4 - 1.039\delta^{exp.} \quad (\text{RMSD} = 3.5\,\text{ppm}). \tag{15}$$

Likewise, linear-regression parameters were obtained for the individual carbon species as summarized in Eqs. (16)–(18):

$$\sigma^{cluster,opt.}_{aliphatic} = 187.0 - 1.052\delta^{exp.} \quad (\text{RMSD} = 2.3\,\text{ppm}), \tag{16}$$

$$\sigma^{cluster,opt.}_{aromatic} = 186.2 - 1.038\delta^{exp.} \quad (\text{RMSD} = 4.6\,\text{ppm}), \tag{17}$$

$$\sigma^{cluster,opt.}_{carboxylic} = 186 - 1.03\delta^{exp.} \quad (\text{RMSD} = 4.3\,\text{ppm}). \tag{18}$$

It should be noted that the optimized and un-optimized are essentially in agreement. The RMSD associated with the structure where all atomic positions were refined is slightly higher than the structures where only the hydrogen positions were refined, except for carboxylic sites, which were modestly improved. Notably, the RMSD of σ_{22} values of carboxylic sites decreases from 5.5 ppm to 4.9 ppm when optimization is performed. In this case, we attribute the improvement to a better representation of the hydrogen bonds. We

conclude that the positions of hydrogen sites that do not participate in hydrogen bonds can be refined using partial optimizations involving isolated molecules and that introducing reorientations of the structure around the heavy atoms sometimes degrades the quality of the structural data except in cases where intermolecular hydrogen-bonding is present.

Some of the largest differences between calculated and experimental chemical-shift values can be attributed to motional averaging. Rovibrational effects tend to reduce calculated chemical-shift anisotropies by averaging over many possible orientations.[107] In the majority of cases where large residuals were encountered in this study, the calculated residuals for σ_{11} and σ_{33} had opposite signs. It is possible to address internal rotations by averaging over a series of single-point chemical-shielding calculations for structures derived from either classical or *ab initio* molecular dynamics (MD) simulations, whether the intermolecular effects are considered as part of a microcanonical or a canonical ensemble. The former method has been employed to study the effects of solvation on the chemical shielding of ions, whereas the latter has been used to account for motion in crystalline systems or proteins.[107–109] Similar methods were employed by Barich *et al.* to study the effects of internal rotations and librations of phenyl rings in biphenyl.[110] In the case of ibuprofen, multi-point studies have been used to improve the correlation with experiment by introducing thermal motion in the form of librations in the phenyl ring and bending modes for the C–H bonds.[92]

The largest discrepancies between experimental principal components and calculated principal components using cluster models for carboxylic sites are for the components whose principal axes lie nearest to the hydrogen bonding axis. These large deviations can be explained by assuming a dynamic effect involving the hydrogen atoms. σ_{11} values for carboxylic sites improved substantially following plane-wave geometry optimizations.

As another example, σ_{22} for aromatic carbons cannot be calculated as accurately as the other two components. It has previously been suggested that large residuals associated with σ_{22} may result from motion of the C–H bond.[94] In nearly every case, the calculated values of σ_{22} are slightly smaller than the experimental value. Furthermore, the agreement of calculated σ_{11} values for aromatic carbons with experimental chemical shifts is generally worse when one includes intermolecular effects and is only marginally improved by geometry optimizations. This observation suggests that rovibrational effects influence this principal component at least as strongly as intermolecular effects.

IV. CONCLUSIONS

The inclusion of intermolecular effects on calculated chemical shielding has been evaluated using density-functional theory for a representative set of organic materials having well-defined atomic coordinates and experimental chemical-shift-tensor components. Molecular clusters and isolated molecules were used to model the solid materials. A comparison of the calculations for the two models shows that cluster models, when properly chosen to take into account the properties of the material, provide systematic improvement over the results of the isolated-molecule model.

One aspect of the problem which this investigation emphasizes is that, with cluster models, one can partition the model structure into regions with locally dense basis sets and regions with lesser basis sets. This approximation greatly reduces the computational cost without a significant effect on the calculated chemical shielding. Such a method allows calculations to be performed on larger clusters, which would otherwise be prohibitively expensive. We find that chemical shielding is strongly influenced by cluster size but that shielding tends to converge smoothly when the number of molecules in the cluster is increased. Clusters that provide converged or nearly converged results can be handled with current software capabilities.

Our analysis demonstrates the importance of size and symmetry considerations when defining a molecular cluster. Clusters should not be defined arbitrarily so that, for instance, only molecules participating in direct hydrogen bonds are included because this may exclude other important intermolecular interactions. Instead, clusters should be defined so as to reflect the crystalline space group. Judicious placement of molecules in a cluster to represent the solid state seems to be of considerable importance in obtaining quantitative results.

The results here strongly suggest that modelling the solid state with extended molecular clusters is a viable alternative to the use of PBCs. Cluster models have several inherent advantages over the latter, including the ability to compare results to isolated-molecule calculations, the possibility of simplification of calculation by using lower basis sets in regions removed from the molecule of interest, general applicability to non-periodic systems, and the ability to use additional model chemistries such as hybrid exchange-correlation functionals and *ab initio* methods.

The crystal structures of acetaminophen, adenosine, ibuprofen, and α-glycine appear to be of poorer quality than the others in this study, based on the frequency of large residuals between calculation and experiment. However, density plane-wave optimizations did not improve the quality of the agreement between experiment and calculation on these molecules. We note that some of the highest residuals have been attributed to rovibrational mechanisms in previous work.[94] It may be possible to assess the importance of rovibrational effects on chemical shielding by employing a series of single-point calculations that describe the motion of the crystalline lattice.

ACKNOWLEDGMENTS

We acknowledge the Pennsylvania State University Center for Nanoscale Science for access to Accelrys MATERIALS STUDIO and use of the Lionxj cluster. We thank Mr. Fahri Alkan for helpful discussions. C.D. acknowledges the support of the National Science Foundation under Grant CHE-0956006 and K.T.M. acknowledges the support of the National Science Foundation under Grant CHE-1213451.

[1] J. C. Facelli, Prog. Nucl. Magn. Reson. Spectrosc. **58**(3), 176–201 (2011).
[2] C. J. Jameson, Annu. Rev. Phys. Chem. **47**(1), 135–169 (1996).

[3]J. Kempf, H. W. Spiess, U. Haeberlen, and H. Zimmermann, Chem. Phys. Lett. **17**(1), 39–42 (1972).
[4]J. Herzfeld and A. E. Berger, J. Chem. Phys. **73**(12), 6021–6030 (1980).
[5]D. W. Alderman, G. McGeorge, J. Z. Hu, R. J. Pugmire, and D. M. Grant, Mol. Phys. **95**(6), 1113–1126 (1998).
[6]J. C. C. Chan and R. Tycko, J. Chem. Phys. **118**(18), 8378–8389 (2003).
[7]D. M. Grant, F. Liu, R. J. Iuliucci, C. G. Phung, J. C. Facelli, and D. W. Alderman, Acta Crystallogr., Sect. B **B51**(4), 540–546 (1995).
[8]J. C. Facelli, D. M. Grant, and J. Michl, Acc. Chem. Res. **20**(4), 152–158 (1987).
[9]M. Kaupp, M. Bühl, and V. G. Malkin, *Calculation of NMR and EPR Parameters: Theory and Applications* (Wiley, 2006).
[10]J. Vaara, Phys. Chem. Chem. Phys. **9**(40), 5399–5418 (2007).
[11]J. C. Facelli, Concepts Magn. Reson., Part A **20A**(1), 42–69 (2004).
[12]A. M. Orendt and J. C. Facelli, in *Annual Reports on NMR Spectroscopy*, edited by G. A. Webb (Elsevier Academic Press Inc, San Diego, 2007), Vol. 62, pp. 115–178.
[13]F. Alkan and C. Dybowski, Phys. Chem. Chem. Phys. **16**(27), 14298–14308 (2014).
[14]C. J. Pickard and F. Mauri, Phys. Rev. B **63**(24), 245101–245113 (2001).
[15]J. C. Johnston, R. J. Iuliucci, J. C. Facelli, G. Fitzgerald, and K. T. Mueller, J. Chem. Phys. **131**(14), 144501–144511 (2009).
[16]C. Bonhomme, C. Gervais, F. Babonneau, C. Coelho, F. Pourpoint, T. Azais, S. E. Ashbrook, J. M. Griffin, J. R. Yates, F. Mauri, and C. J. Pickard, Chem. Rev. **112**(11), 5733–5779 (2012).
[17]A. D. Becke, J. Chem. Phys. **98**(7), 5648–5652 (1993).
[18]R. Laskowski, P. Blaha, and F. Tran, Phys. Rev. B **87**(19), 195130 (2013).
[19]A. V. Arbuznikov and M. Kaupp, Int. J. Quant. Chem. **111**(11), 2625–2638 (2011).
[20]R. Suardiaz, C. Perez, R. Crespo-Otero, J. M. G. de la Vega, and J. S. Fabian, J. Chem. Theory Comput. **4**(3), 448–456 (2008).
[21]P. Broqvist, A. Alkauskas, and A. Pasquarello, Phys. Rev. B **80**(8), 085114 (2009).
[22]R. Ditchfield, Mol. Phys. **27**(4), 789–807 (1974).
[23]G. Schreckenbach and T. Ziegler, J. Phys. Chem. **99**(2), 606–611 (1995).
[24]J. R. Cheeseman, G. W. Trucks, T. A. Keith, and M. J. Frisch, J. Chem. Phys. **104**(14), 5497–5509 (1996).
[25]G. Schreckenbach and T. Ziegler, Theor. Chem. Acc. **99**(2), 71–82 (1998).
[26]C. J. Jameson and A. C. de Dios, J. Chem. Phys. **97**(1), 417–434 (1992).
[27]J. F. Hinton, P. Guthrie, P. Pulay, and K. Wolinski, J. Am. Chem. Soc. **114**(5), 1604–1605 (1992).
[28]H. Koller, G. Engelhardt, A. P. M. Kentgens, and J. Sauer, J. Phys. Chem. **98**(6), 1544–1551 (1994).
[29]J. A. Tossell, J. Magn. Reson. **127**(1), 49–53 (1997).
[30]J. A. Tossell, Chem. Phys. Lett. **303**(3–4), 435–440 (1999).
[31]J. A. Tossell, Phys. Chem. Miner. **27**(1), 70–80 (1999).
[32]G. Valerio, A. Goursot, R. Vetrivel, O. Malkina, V. Malkin, and D. R. Salahub, J. Am. Chem. Soc. **120**(44), 11426–11431 (1998).
[33]G. Valerio and A. Goursot, J. Phys. Chem. B **103**(1), 51–58 (1999).
[34]S.-H. Cai, Z. Chen, and H.-L. Wan, J. Phys. Chem. A **106**(6), 1060–1066 (2002).
[35]M. Body, G. Silly, C. Legein, and J.-Y. Buzare, J. Phys. Chem. B **109**(20), 10270–10278 (2005).
[36]O. Dmitrenko, S. Bai, P. A. Beckmann, S. van Bramer, A. J. Vega, and C. Dybowski, J. Phys. Chem. A **112**(14), 3046–3052 (2008).
[37]O. Dmitrenko, S. Bai, and C. Dybowski, Solid State Nucl. Magn. Reson. **34**(3), 186–190 (2008).
[38]A. M. Orendt, J. C. Facelli, and D. M. Grant, Chem. Phys. Lett. **302**(5–6), 499–504 (1999).
[39]G. Zheng, L. Wang, J. Hu, X. Zhang, L. Shen, C. Ye, and G. A. Webb, Magn. Reson. Chem. **35**(9), 606–608 (1997).
[40]J. Z. Hu, J. C. Facelli, D. W. Alderman, R. J. Pugmire, and D. M. Grant, J. Am. Chem. Soc. **120**(38), 9863–9869 (1998).
[41]M. S. Solum, K. L. Altman, M. Strohmeier, D. A. Berges, Y. Zhang, J. C. Facelli, R. J. Pugmire, and D. M. Grant, J. Am. Chem. Soc. **119**(41), 9804–9809 (1997).
[42]J. C. Facelli, R. J. Pugmire, and D. M. Grant, J. Am. Chem. Soc. **118**(23), 5488–5489 (1996).
[43]X. Chen and C.-G. Zhan, J. Mol. Struct. **682**(1–3), 73–82 (2004).
[44]J. Weber and J. S. Auf der Gunne, Phys. Chem. Chem. Phys. **12**(3), 583–603 (2010).
[45]J. A. Pople, Proc. R. Soc. London, Ser. A **239**, 541–549 (1957).
[46]J. A. Pople, Proc. R. Soc. London, Ser. A **239**, 550–556 (1957).
[47]N. F. Ramsey, Phys. Rev. **78**(6), 699–703 (1950).
[48]N. F. Ramsey, Phys. Rev. **77**(4), 567–567 (1950).
[49]J. A. Pople, J. Chem. Phys. **37**(1), 53–59 (1962).
[50]C. M. Widdifield and R. W. Schurko, Concepts Magn. Reson., Part A **34A**(2), 91–123 (2009).
[51]F. Liu, C. G. Phung, D. W. Alderman, and D. M. Grant, J. Am. Chem. Soc. **118**(43), 10629–10634 (1996).
[52]G. A. Jeffrey, R. K. McMullan, and S. Takagi, Acta Crystallogr., Sect. B **B33**(3), 728–737 (1977).
[53]S. Takagi and G. A. Jeffrey, Acta Crystallogr., Sect. B **B35**(4), 902–906 (1979).
[54]S. Takagi and G. A. Jeffrey, Acta Crystallogr., Sect. B **B34**(6), 2006–2010 (1978).
[55]S. Takagi and G. A. Jeffrey, Acta Crystallogr., Sect. B **B33**(10), 3033–3040 (1977).
[56]M. H. Sherwood, D. W. Alderman, and D. M. Grant, J. Magn. Reson., Ser A **104**(2), 132–145 (1993).
[57]G. M. Brown and H. A. Levy, Acta Crystallogr., Sect. B **29**(4), 790–797 (1973).
[58]F. Liu, C. G. Phung, D. W. Alderman, and D. M. Grant, J. Magn. Reson., Ser A **120**(2), 242–248 (1996).
[59]S. Takagi and G. A. Jeffrey, Acta Crystallogr., Sect. B **B34**(8), 2551–2555 (1978).
[60]F. Liu, C. G. Phung, D. W. Alderman, and D. M. Grant, J. Magn. Reson., Ser A **120**(2), 11–11 (1996).
[61]S. Takagi and G. A. Jeffrey, Acta Crystallogr., Sect. B **B33**(11), 3510–3515 (1977).
[62]V. G. Malkin, O. L. Malkina, and D. R. Salahub, J. Am. Chem. Soc. **117**(11), 3294–3295 (1995).
[63]P. G. Jonsson and A. Kvick, Acta Crystallogr., Sect. B **28**(Pt. 6), 1827–1833 (1972).
[64]M. J. Potrzebowski, P. Tekely, and Y. Dusausoy, Solid State Nucl. Magn. Reson. **11**(3–4), 253–257 (1998).
[65]A. Kvick, W. M. Canning, T. F. Koetzle, and G. J. B. Williams, Acta Crystallogr., Sect. B **36**(1), 115–120 (1980).
[66]A. Naito, S. Ganapathy, K. Akasaka, and C. A. McDowell, J. Chem. Phys. **74**(6), 3190–3197 (1981).
[67]C. C. Wilson, D. Myles, M. Ghosh, L. N. Johnson, and W. Wang, New J. Chem. **29**(10), 1318–1322 (2005).
[68]A. Naito, S. Ganapathy, P. Raghunathan, and C. A. McDowell, J. Chem. Phys. **79**(9), 4173–4182 (1983).
[69]M. N. Frey, M. S. Lehmann, T. F. Koetzle, and W. C. Hamilton, Acta Crystallogr., Sect. B **29**(Pt. 4), 876–884 (1973).
[70]A. Naito and C. A. McDowell, J. Chem. Phys. **81**(11), 4795–4803 (1984).
[71]M. Ramanadham, S. K. Sikka, and R. Chidambaram, Acta Crystallogr., Sect. B **28**(Pt. 10), 3000–3005 (1972).
[72]N. Janes, S. Ganapathy and E. Oldfield, J. Magn. Reson. **54**(1), 111–121 (1969).
[73]M. Ramanadham, S. K. Sikka, and R. Chidambaram, Pramana **1**(6), 247–259 (1973).
[74]R. G. Griffin, A. Pines, S. Pausak, and J. S. Waugh, J. Chem. Phys. **63**(3), 1267–1271 (1975).
[75]T. M. Sabine, G. W. Cox, and B. M. Craven, Acta Crystallogr., Sect. B **25**(Pt. 12), 2437–2441 (1969).
[76]M. Mehring and J. D. Becker, Phys. Rev. Lett. **47**(5), 366–370 (1981).
[77]D. Semmingsen, F. J. Hollander, and T. F. Koetzle, J. Chem. Phys. **66**(10), 4405–4412 (1977).
[78]M. H. Sherwood, J. C. Facelli, D. W. Alderman, and D. M. Grant, J. Am. Chem. Soc. **113**(3), 750–753 (1991).
[79]S. C. Capelli, A. Albinati, S. A. Mason, and B. T. M. Willis, J. Phys. Chem. A **110**(41), 11695–11703 (2006).
[80]S. Pausak, A. Pines, and J. S. Waugh, J. Chem. Phys. **59**(2), 591–595 (1973).
[81]E. Prince, L. W. Schroeder, and J. J. Rush, Acta Crystallogr., Sect. B **29**(Pt. 2), 184–191 (1973).
[82]R. J. Iuliucci, C. G. Phung, J. C. Facelli, and D. M. Grant, J. Am. Chem. Soc. **120**(36), 9305–9311 (1998).
[83]G. Ferraris, D. W. Jones, and J. Yerkess, Z. Kristallogr. **138**, 113–128 (1973).
[84]R. J. Iuliucci, J. C. Facelli, D. W. Alderman, and D. M. Grant, J. Am. Chem. Soc. **117**(8), 2336–2343 (1995).
[85]A. C. Hazell, R. G. Hazell, L. Noerskov-Lauritsen, C. E. Briant, and D. W. Jones, Acta Crystallogr., Sect. C **C42**(6), 690–693 (1986).
[86]F. Liu, A. M. Orendt, D. W. Alderman, and D. M. Grant, J. Am. Chem. Soc. **119**(38), 8981–8984 (1997).

[87]D. Semmingsen, Acta Chem. Scand., Ser. A **A42**(5), 279–283 (1988).
[88]D. Stueber and D. M. Grant, J. Am. Chem. Soc. **124**(35), 10539–10551 (2002).
[89]W. T. Klooster, J. R. Ruble, B. M. Craven, and R. K. McMullan, Acta Crystallogr., Sect. B **B47**(3), 376–383 (1991).
[90]J. K. Harper, R. Iuliucci, M. Gruber, and K. Kalakewich, CrystEngComm **15**(43), 8693–8704 (2013).
[91]C. C. Wilson, J. Mol. Struct. **405**(2–3), 207–217 (1997).
[92]E. Carignani, S. Borsacchi, A. Marini, B. Mennucci, and M. Geppi, J. Phys. Chem. C **115**(50), 25023–25029 (2011).
[93]N. Shankland, C. C. Wilson, A. J. Florence, and P. J. Cox, Acta Crystallogr., Sect. C **C53**(7), 951–954 (1997).
[94]T. H. Sefzik, D. Turco, R. J. Iuliucci, and J. C. Facelli, J. Phys. Chem. A **109**(6), 1180–1187 (2005).
[95]T. H. Sefzik, J. M. Fidler, R. J. Iuliucci, and J. C. Facelli, Magn. Reson. Chem. **44**(3), 390–400 (2006).
[96]R. K. Harris, P. Hodgkinson, C. J. Pickard, J. R. Yates, and V. Zorin, Magn. Reson. Chem. **45**, S174–S186 (2007).
[97]A. D. Becke, J. Chem. Phys. **98**(2), 1372–1377 (1993).
[98]C. Lee, W. Yang, and R. G. Parr, Phys. Rev. B **37**(2), 785–789 (1988).
[99]P. C. Hariharan and J. A. Pople, Chem. Phys. Lett. **16**(2), 217–219 (1972).
[100]S. J. Clark, M. D. Segall, C. J. Pickard, P. J. Hasnip, M. J. Probert, K. Refson, and M. C. Payne, Z. Kristallogr, **220**(5–6), 567–570 (2009).
[101]J. P. Perdew, K. Burke, and M. Ernzerhof, Phys. Rev. Lett. **77**(18), 3865–3868 (1996).
[102]J. P. Perdew and Y. Wang, Phys. Rev. B **45**(23), 13244 (1992).
[103]T. H. Dunning, J. Chem. Phys. **90**(2), 1007–1023 (1989).
[104]M. J. Frisch, G. W. Trucks, H. B. Schlegel *et al.*, GAUSSIAN 09, Revision B.01, Gaussian, Inc., Wallingford, CT, 2009.
[105]D. B. Chesnut and K. D. Moore, J. Comput. Chem. **10**(5), 648–659 (1989).
[106]D. B. Chesnut, B. E. Rusiloski, K. D. Moore, and D. A. Egolf, J. Comput. Chem. **14**(11), 1364–1375 (1993).
[107]M. Dracinsky and P. Hodgkinson, CrystEngComm **15**(43), 8705–8712 (2013).
[108]L. A. Truflandier and J. Autschbach, J. Am. Chem. Soc. **132**(10), 3472–3483 (2010).
[109]C. Scheurer, N. R. Skrynnikov, S. F. Lienin, S. K. Straus, R. Bruschweiler, and R. R. Ernst, J. Am. Chem. Soc. **121**(17), 4242–4251 (1999).
[110]D. H. Barich, R. J. Pugmire, D. M. Grant, and R. J. Iuliucci, J. Phys. Chem. A **105**(28), 6780–6784 (2001).